

Computation of Cross-sections by Effects of Theoretical Parameters Code for Production of ^{52}Mn Radioisotope

Glara F. Hasan^{a,b,c}, Edrees. M. Harki^{a,d} and Flavia Groppi^{b,c}

^a Department of Physics, College of Education, University of Salahaddin, Erbil, Kurdistan Region, Iraq.

^b Department of Physics, Università degli Studi di Milano, via Celoria 16, I-20133 Milano, Italy.

^c Laboratorio Acceleratori e Superconduttività Applicata (LASA), Department of Physics, Università degli Studi di Milano and Istituto Nazionale di Fisica Nucleare (INFN)-Milano, via F.lli Cervi 201, I-20090 Segrate (MI), Italy.

^d Technical Engineering College, Erbil Polytechnic University, Erbil, 44001, Kurdistan region, Iraq.

Doi: <https://doi.org/10.47011/16.5.1>

Received on: 05/11/2021;

Accepted on: 14/06/2022

Abstract: Theoretical calculations focusing on cross-section data results for the production of ^{52}Mn from a natural chromium (^{nat}Cr) target have been investigated for deuteron beams up to 35 MeV by using the EMPIRE 3.2.2 Malta nuclear model code. The optimization of theoretical calculations is important for the medical production routes of cross-section isotopes. In these computations, we tested different ATILNO parameters for the evaluation of cross-section data and improved techniques for the theoretical calculation of radioisotope ^{52}Mn . The effects of these parameters were investigated, and the theoretical results were subsequently compared with each other, existing literature data, and the TENDL-2019 library.

Keywords: EMPIRE code, Cross-section, Manganese-52, Radionuclide production, Positron emission tomography.

1. Introduction

Knowledge of the diagnostic imaging techniques in nuclear medicine is important for rapid progress [1]. A large number of radiopharmaceuticals are used in nuclear medicine (NM) for diagnostic purposes. One of the most important imaging techniques that uses radioactive materials is positron emission tomography (PET) [2, 3], which uses radioactive sources as radiotracers to visualize and measure changes in physiological activities and metabolic processes [4]. Calculating the cross-section data of a nucleus is a fundamental concept in predicting the probability of a nuclear reaction. The EMPIRE program is one of the most preferred codes used for various nuclear

reactions and incident particle types and energy. In addition, in this simulation code, the relationship of the properties of the target to the computation of cross-sections can be used to improve the nuclear model data and predict unknown nuclear data [5, 6]. The main objective of this work is to investigate the effect of one of the input parameters of the theoretical program on the cross-section production of the important medical radioisotope $^{52\text{g,cum}}\text{Mn}$. Manganese possesses three positron-emitting isotopes with appropriate half-lives, making it suitable for application as a PET tracer. ^{52}Mn 5.591 d, $^{52\text{m}}\text{Mn}$ (21.1 min), and ^{51}Mn (46.2 min) due to its low positron energy and range in tissue for ^{52}Mn are

(244.6 keV, 0.63mm), ^{52m}Mn (1179 keV, 5.288 mm) and ^{51}Mn (970.2 keV, 4.275 mm). Their lowest energy is ^{52}Mn (244.6 keV, 0.63 mm) [7, 8], which is comparable to the most common PET radiotracer ^{18}F (250 keV, 0.62 mm). The results for fluorine-18 (^{18}F) closely resemble those of ^{52}Mn . Given the smaller positron ranges of both ^{52}Mn and ^{18}F , they contribute to enhanced resolution in PET scanners [9]. ^{52}Mn can be studied cross-sections by using deuteron energy beams, with natural chromium targets including natural composition (^{50}Cr : 4.345%; ^{52}Cr : 83.789%; ^{53}Cr : 9.501%; ^{54}Cr : 2.365%) [10]. It is, therefore, necessary to know that under our conditions for the computation of cross-sections for ^{52}Mn , it was impossible to make an experimental measurement of the contribution of the short half-life metastable level ($t_{1/2} = 21.1$ m) that decays to the longer ground state by isomeric transition (IT) (1.68 %). In this case, theoretically determined cross-section is relative to the cumulative activation production of ^{52g}Mn after total decay of its isomer. The EMPIRE 3.2.2 code was employed for the reaction $^{\text{nat}}\text{Cr}(d,xn)^{52g,\text{cum}}\text{Mn}$. The obtained cross-section results from various computational codes, using different input parameters, were compared with literature databases and TENDL-2019 [11].

2. Computational details

2.1 Theoretical Calculations Code

Theoretical calculations came to the forefront because they provide a good predictive ability for researchers without the difficulties of experimental drawbacks, such as financial and time constraints. In this study, we employed the EMPIRE 3.2.2 Malta code, an advanced system of nuclear reaction codes for the simulation of various nuclear models and incident particles across different energy ranges of the reaction mechanisms [5]. Given the significant impact of input parameters on cross-section improvements, adjustments were made to achieve a robust alignment with the experimental data. A crucial factor in the EMPIRE code, related to level density, is the ATILNO factor, which can be controlled from the input parameters. To obtain good match results, we used the default and three other values of ATILNO (0, 0.7, 1, and 1.3) alongside other essential parameters, including optical model parameters (OMP), selected from the Reference Input Parameter Library (RIPL-3).

Additionally, we computed the OMP following the approach outlined by Anand and Cai [12] and set the level density model (LEV DEN) to the generalized superfluid model (GSM).

2.2 TENDL-2019 Library

TENDL-2019, the latest version of TENDL, uses the nuclear model code TALYS as a nuclear data library that provides an output of the TALYS code system in the Evaluated Nuclear Data File (ENDF) format. The online TENDL-2019 library is the tenth version of the TENDL data libraries. The TENDL-2019 library includes sub-libraries for bombarding photons, protons, neutrons, deuterons, tritons, ^3He , and ^4He particles, covering 2,800 isotopes up to 200 MeV [11].

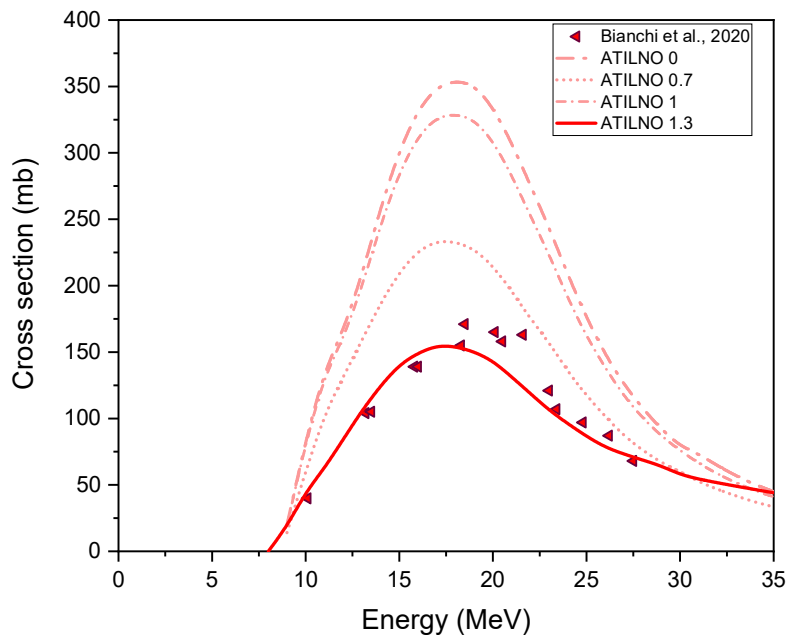
3. Results and Discussions

The theoretical cross-sections computed for the medical radioisotope ^{52}Mn have been studied at different values of ATILNO (0, 0.7, 1, and 1.3) by the EMPIRE 3.2.2 Malta code in the deuteron energy, by considering how the results change with different values of ATILNO. The computation results obtained by the EMPIRE 3.2.2 code for the nuclear reaction $^{\text{nat}}\text{Cr}(d,xn)^{52g,\text{cum}}\text{Mn}$ are reported in Table 1 and represented in Fig. 1 with the comparison with our experimental results [13].

We can conclude from Fig. 1 that with the default program in which ATILNO is zero, the results are very different from all experimental and TENDL-2019 data sets. For this reason, we decided to optimize the input for a certain number of ATILNO parameters between 0.7 and 1.3. Each of the ATILNO parameter results produces significantly different results in the cross-section. In this work, we have decided to apply the selection of ATILNO = 1.3 with the configuration of the parameters fixed level density to the generalized superfluid model (GSM) values. We selected the optical model parameters by Anand and Cai [12]. By proving this input parameter, we obtained the best results and compared them with our experimental results, other experimental data sets, and TENDL-2019.

TABLE 1. Calculated cross-sections (mb) for $^{\text{nat}}\text{Cr}(d,x)^{52}\text{g,cumMn}$, related to three different values of ATILNO of the EMPIRE 3.2.2 code.

Energy(MeV)	$^{52}\text{g,cum Mn}$ (mb)	$^{52}\text{g,cum Mn}$ (mb)	$^{52}\text{g,cum Mn}$ (mb)	$^{52}\text{g,cum Mn}$ (mb)
	ATILNO 0	ATILNO 0.7	ATILNO 1	ATILNO 1.3
9	20.15	14.01	19.74	18.95
10	83.33	60.31	81.3	44.51
11	136.06	102.55	131.97	62.47
12	165.85	131.34	159.95	84.25
13	207.64	158.69	198.66	105.83
14	258.50	186.80	245.67	124.59
15	301.79	210.05	285.19	140.51
16	332.48	226.39	312.62	149.27
17	349.89	233.68	327.06	154.98
18	354.51	233.02	329.34	154.23
19	351.30	227.68	325.22	150.28
20	334.51	214.88	309.18	143.36
21	307.68	19.20	283.25	131.3
22	275.47	175.08	252.53	118.86
23	243.87	157.37	223.71	106.23
24	208.109	135.35	190.52	96.15
25	175.87	117.22	161.81	86.63
26	148.14	101.55	138.21	78.34
27	125.76	87.06	116.93	73.23
28	207.55	75.93	100.29	68.72
29	91.88	66.74	86.83	64.24
30	79.21	59.53	75.80	57.81
31	73.27	52.39	66.20	54.37
32	64.42	46.54	58.22	51.56
33	56.84	41.64	51.52	49.05
34	50.15	36.93	45.63	46.53
35	44.95	33.55	40.98	44.06


 FIG. 1. Computation results of the EMPIRE 3.2.2 code for the optimized production of $^{52}\text{g,cumMn}$ by nuclear reaction $^{\text{nat}}\text{Cr}(d,x)^{52}\text{g,cumMn}$.

3.1 Cross-section of ${}^{\text{nat}}\text{Cr}(d,xn){}^{52\text{g,cum}}\text{Mn}$

The theoretical cross-sections computed for the production of medical radioisotope ${}^{52\text{g,cum}}\text{Mn}$ with incident deuteron energy up to 35 MeV have been studied by several authors [13-21]. Figure 2 presents the optimized results for the cross-sections involved in different ATILNO values. The obtained results were compared with the existing experimental cross-section data and the data taken from TENDL-2019.

The computation was carried out using various ATILNO (0, 0.7, 1, and 1.3) values for the production of ${}^{52\text{g,cum}}\text{Mn}$. As shown in Figure 1, the production of ${}^{52\text{g,cum}}\text{Mn}$ exhibits diverse values of cross-sections corresponding to each different ATILNO. In our experimental group, the focus was on calculating the cross-section contribution to the total decay of cumulative ${}^{52\text{g}}\text{Mn}$. Therefore, the theoretical data was employed to represent the experimental for the purpose of calculation. The theoretical results were obtained by considering weighted cross-section contributions derived from the deuteron

reactions for natural chromium ${}^{\text{nat}}\text{Cr}$, which consists of ${}^{50,52,53,54}\text{Cr}$ isotopes. The contribution of ${}^{50}\text{Cr}$ across all energy ranges is very close to zero and has been ignored. For ${}^{52}\text{Cr}$, constituting the majority at 83.789% of natural abundance, the contribution is predominant across all ATILNO parameters and reaches the maximum at 154.98 mb at 17 MeV. In the case of ${}^{53}\text{Cr}$, its contribution is zero up to 16 MeV, and for ${}^{54}\text{Cr}$, it is zero up to 27 MeV.

It should be noted that the achieved EMPIRE prediction is in good agreement with experimental data, demonstrating a consistent curve shape. Specifically, in this instance, we selected ATILNO 1.3. It is clearly seen that the cross-section results for ATILNO 0 and 1 exhibit substantial differences in magnitude and show data that is higher compared to all the experimental data sets. Conversely, the results for ATILNO 0.7 show good agreement solely with TENDL-2019, with the curve registering higher than other experimental data sets.

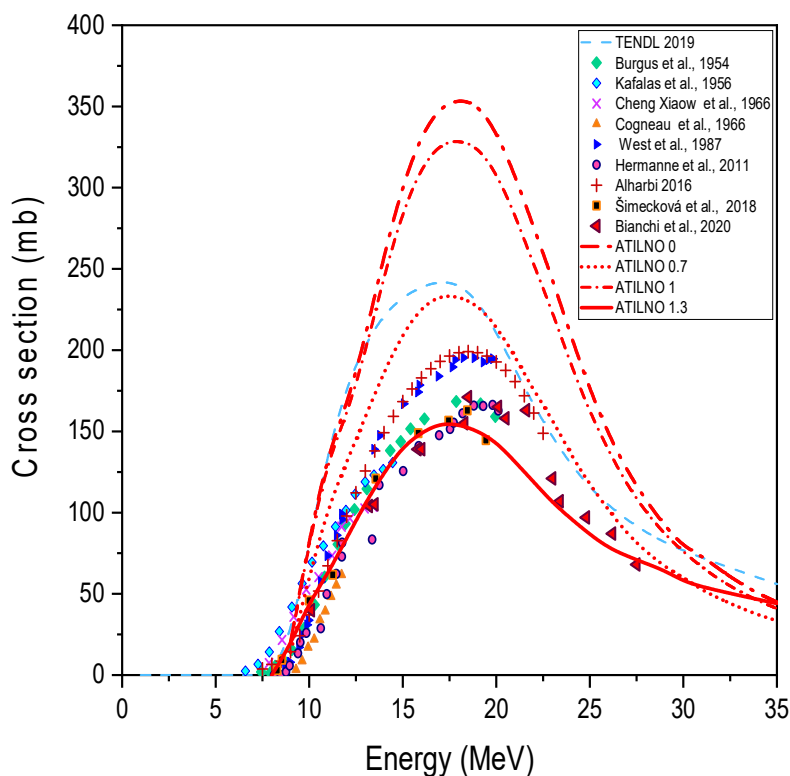


FIG. 2. Computation results of the EMPIRE 3.2.2 code by different ATILNO values for ${}^{\text{nat}}\text{Cr}(d,xn){}^{52\text{g,cum}}\text{Mn}$, compared with the experimental data sets present in the literature and TENDL.

4. Conclusion

The results presented in Figures 1 and 2 indicate very good agreement between the data obtained in this study and other experimental

data available in the literature. This can be summarized as the investigated reactions and the maximum production cross-section values of the ${}^{52\text{g,cum}}\text{Mn}$, are achieved at 154.98 mb with maximum cross-section energy of 17 MeV. In

these computations using the EMPIRE code, the best match is obtained by adjusting the input parameter ATILNO to 1.3, as depicted in Figs. 1 and 2.

These findings contribute significantly to the improvement of theoretical nuclear models and radioisotope production routes. To enhance the accuracy and predictability of various radioisotopes used in nuclear medicine (NM),

one must consider that the ATILNO factor affects the cross-section calculation results. The EMPIRE code's predictive power is demonstrated by analyzing computing results with various experimental observables. Our goal was to demonstrate the suitability of the EMPIRE code for applications related to radioisotopes used in PET medical imaging.

References

- [1] Sekerciand, M. and Özdoğan, H., *HNPS Adv. Nucl. Phys.*, 27 (2020) 68.
- [2] Bailey, D.L., Maisey, M.N., Townsend, D.W., and Valk, P.E., "Positron Emission Tomography", (Springer, 2005).
- [3] Chen, D., Yang, D., Dougherty, C.A., Lu, W., Wu, H., He, X., Cai, T., Van Dort, M.E., Ross, B.D., and Hong, H., *ACS Nano*, 11 (2017) 4315.
- [4] Davidson, C.Q., Phenix, C.P., Tai, T., Khaper, N., and Lees, S.J., *Am. J. Nucl. Med. Mol. Imaging*, 8 (2018) 200.
- [5] Herman, M., Capote, R., Carlson, B., Obložinský, P., Sin, M., Trkov, A., Wienke, H., and Zerkin, V., *Nucl. Data Sheets*, 108 (2007) 2655.
- [6] Herman, M., Capote, R., Sin, M., Trkov, A., Carlson, B., Obložinský, P., Mattoon, C., Wienke, H., and Hoblit, S., "EMPIRE-3.2 Malta modular system for nuclear reaction calculations and nuclear data evaluation", User's Manual, (Brookhaven National Laboratory (BNL) National Nuclear Data Center, 2013).
- [7] Firestone, R.B., Baglin, C.M., and Chu, S., "Table of Isotopes", (Number Bd. 4, Wiley, 1999).
- [8] Conti, M. and Eriksson, L., *EJNMMI Phys.*, 3 (2016) 1.
- [9] Pagani, M., Stone-Elander, S., and Larsson, S.A., *Eur. J. Nucl. Med.*, 24 (1997) 1301.
- [10] Magill, J., Galy, J., and Pfennig, G., "Karlsruher Nuklidkarte", (Haberbeck, 2012).
- [11] Koning, A., Rochman, D., Sublet, J.-C., Dzysiuk, N., Fleming, M., and Van der Marck, S., *Nucl. Data Sheets*, 155 (2019) 1.
- [12] Anand, H. and Cai, C., *Phys. Rev. C*, 73 (2006) 054605.
- [13] Bianchi, F., Marchi, C., Fuad, G., Groppi, F., Haddad, F., Magagnin, L., and Manenti, S., *Appl. Radiat. Isotopes*, 166 (2020) 109329.
- [14] Burgus, W.H., Cowan, G.A., Hadley, J., Hess, W., Shull, T., Stevenson, M., and York, H., *Phys. Rev.*, 95 (1954) 750.
- [15] Kafalasand, P. and Irvine Jr, J.W., *Phys. Rev.*, 104 (1956) 703.
- [16] Cogneau, M., Gilly, L., and Cara, J., *Nucl. Phys.*, 79 (1966) 203.
- [17] Xiaowu, C., Zhenxia, W., Zhenjie, W., and Jinqing, Y., *Acta Phys. Sin.*, 22 (1966) 250.
- [18] West Jr, H., Lanier, R., and Mustafa, M., *Phys. Rev. C*, 35 (6) (1987) 2067.
- [19] Hermanne, A., Rebeles, R.A., Tárkányi, F., Takacs, S., Takács, M., and Ignatyuk, A., *Nucl. Instrum. Meth. B*, 269 (2011) 2563.
- [20] Alharbi, A., *Arab J. Nucl. Sci. Appl.*, 94 (2016) 216.
- [21] Simeckova, E., Avrigeanu, M., Fischer, U., Mrazek, J., Novak, J., Stefanik, M., Costache, C., and Avrigeanu, V., *Phys. Rev. C*, 98 (2018) 034606.